Electronic Supplementary Information (ESI)

Li-Ion Hopping Conduction in Highly Concentrated Lithium Bis(fluorosulfonyl)amide/Dinitrile Liquid Electrolytes

Yosuke Ugata,[a] Morgan L. Thomas,[a,§] Toshihiko Mandai,[b,c] Kazuhide Ueno,[a] Kaoru Dokko,[a,d,*] and Masayoshi Watanabe [a]

[a] Department of Chemistry and Biotechnology, Yokohama National University, 79-5 Tokiwadai, Hodogaya-ku, Yokohama 240-8501, Japan

[b] Department of Chemistry and Biological Science Studies in Chemistry, Iwate University, Ueda 4-3-5, Morioka, 020-8551, Japan

[c] Center for Green Research on Energy and Environmental Materials, National Institute of Materials Science, 1-1 Namiki, Tsukuba, Ibaraki 305-0044, Japan

[d] Unit of Elements Strategy Initiative for Catalysts & Batteries (ESICB), Kyoto University, Kyoto 615-8510, Japan

[§]Present address: Department of Materials and Life Sciences, Faculty of Science and Engineering, Sophia University, 7-1 Kioicho, Chiyoda-ku, Tokyo 102-8554, Japan

*To whom correspondence should be addressed. E-mail: dokko-kaoru-js@ynu.ac.jp

Table S1. Crystallographic data of LiFSA-$(SN)_2$.

	[LiFSA]/[SN] = 1/2
Chemical formula	$C_8H_8F_2LiN_5O_4S_2$
Formula weight	347.24
Crystal system	Monoclinic
Space group	*Pn* (No. 7)
a / Å	13.103(3)
b / Å	12.045(2)
c / Å	14.848(4)
α / °	90
β / °	112.34(3)
γ / °	90
V / Å^3	2167.5(10)
Z	6
D_{calc} / g cm^{-3}	1.596
μ / mm^{-1}	0.4134
Temp. / K	223
Reflections collected	16327
Independent reflection, R_{int}	7655, 0.0450
R_1 [I > 2σ(I)]	0.0782
wR_2 (all data)	0.2867
Goodness of fit	1.125

*The precision of the analysis is not sufficient for registration with Cambridge Structural Database (CSD), thus, the LiFSA-$(SN)_2$ crystal have no CCDC number.

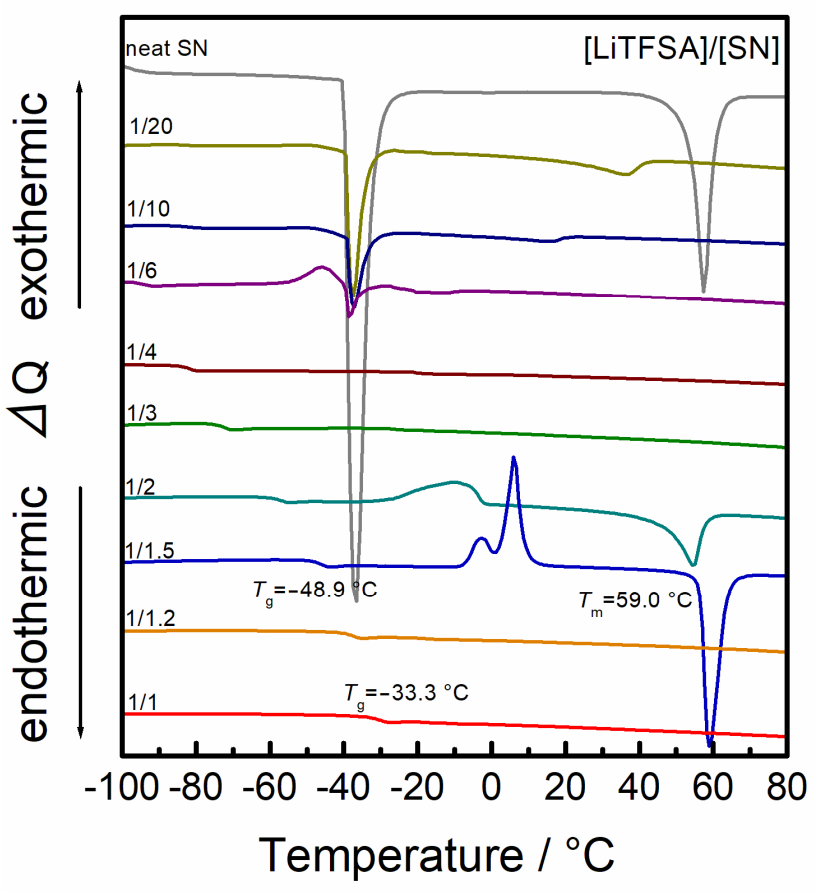

Figure S1. DSC thermograms of binary mixtures of LiTFSA and SN (molar ratio of [LiTFSA]/[SN] = 1/*n*).

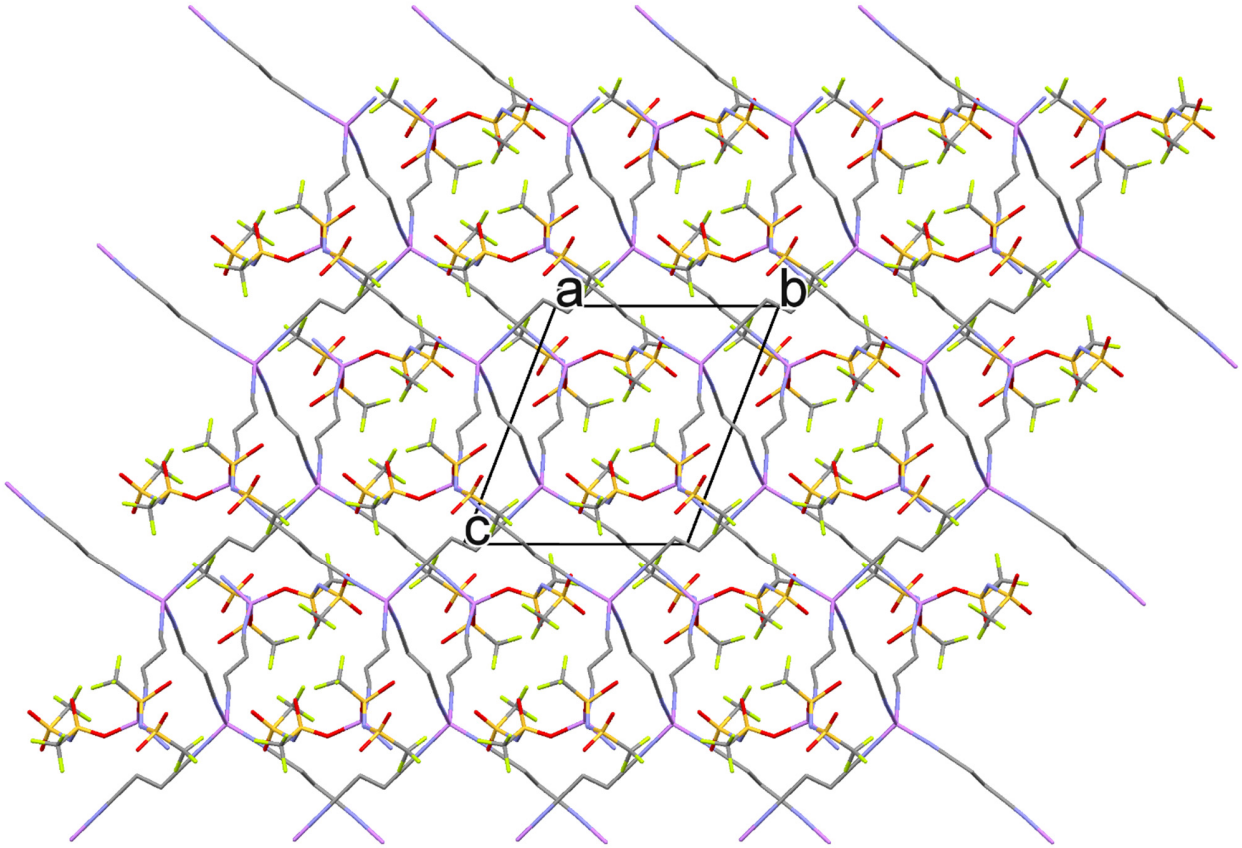

Figure S2. Packing diagram of LiTFSA-$(SN)_{1.5}$ crystal. Disordered atoms are shown in the figure while hydrogen atoms are omitted. Purple, Li; red, O; gray, C; yellow, S; light green, F; lite blue, N. Single crystal of LiTFSA-$(SN)_{1.5}$ was successfully grown in the melt of LiTFSA-$(SN)_{1.5}$ at room temperature.

Table S2. Crystallographic data of LiTFSA-$(SN)_{1.5}$.

	[LiTFSA]/[SN] = 1/1.5
Chemical formula	$C_{16}H_{12}F_{12}Li_2N_8O_8S_4$
Formula weight	814.42
Crystal system	triclinic
Space group	$P\bar{1}$ (No. 2)
a / Å	12.0520(8)
b / Å	12.3787(7)
c / Å	13.2641(8)
α / °	101.687(5)
β / °	105.262(5)
γ / °	115.116(6)
V / Å^3	1612.8(2)
Z	2
D_{calc} / g cm^{-3}	1.677
μ / mm^{-1}	0.4162
Temp. / K	223
Reflections collected	20243
Independent reflection, R_{int}	6895, 0.0235
R_1 [I > 2σ(I)]	0.0752
wR_2 (all data)	0.2477
Goodness of fit	1.050

*The precision of the analysis is not sufficient for registration with Cambridge Structural Database (CSD), thus, the LiTFSA-$(SN)_{1.5}$ crystal have no CCDC number.

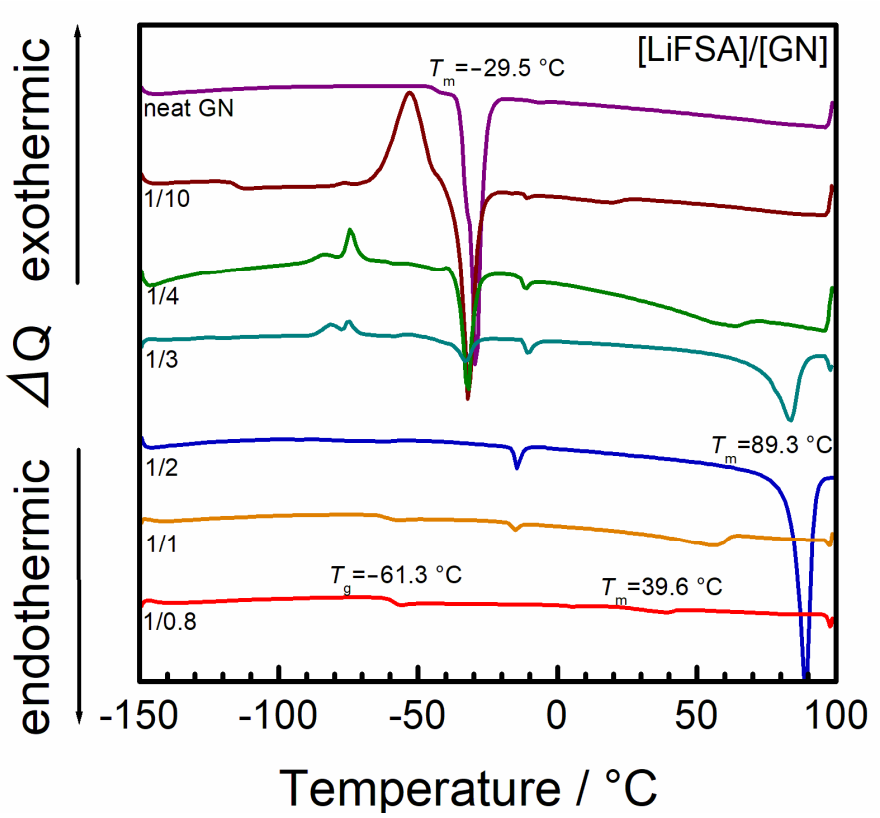

Figure S3. DSC thermograms of binary mixtures of LiFSA and GN (molar ratio of [LiFSA]/[GN] = 1/*n*).

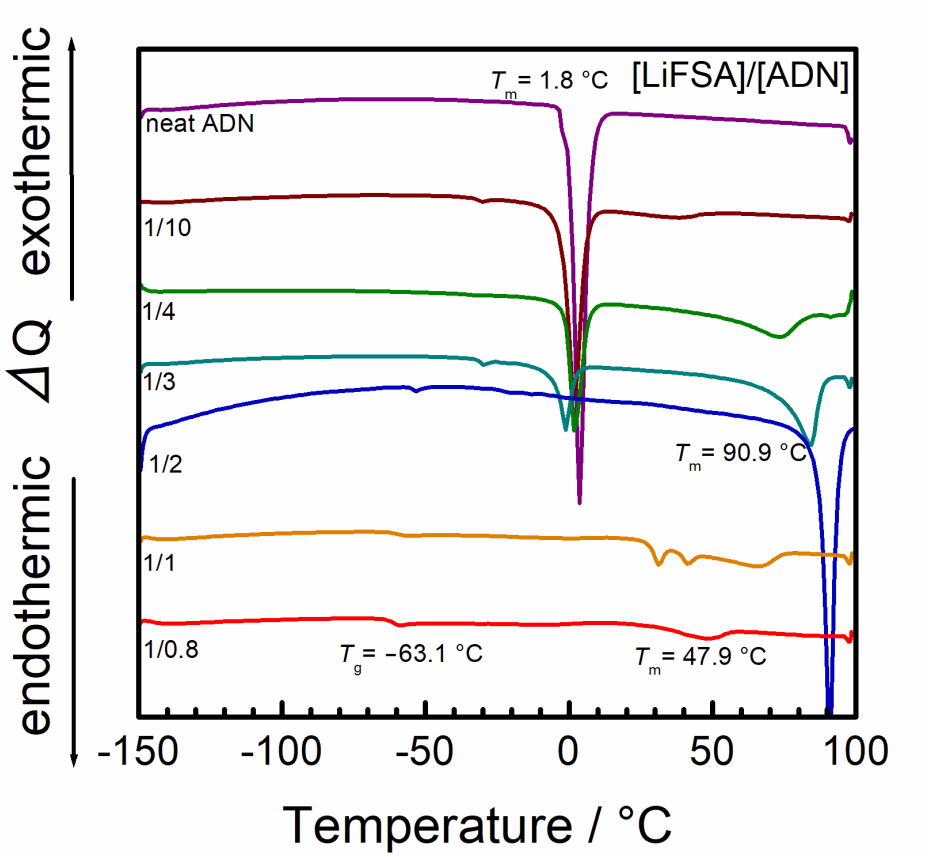

Figure S4. DSC thermograms of binary mixtures of LiFSA and ADN (molar ratio of [LiFSA]/[ADN] = 1/*n*).

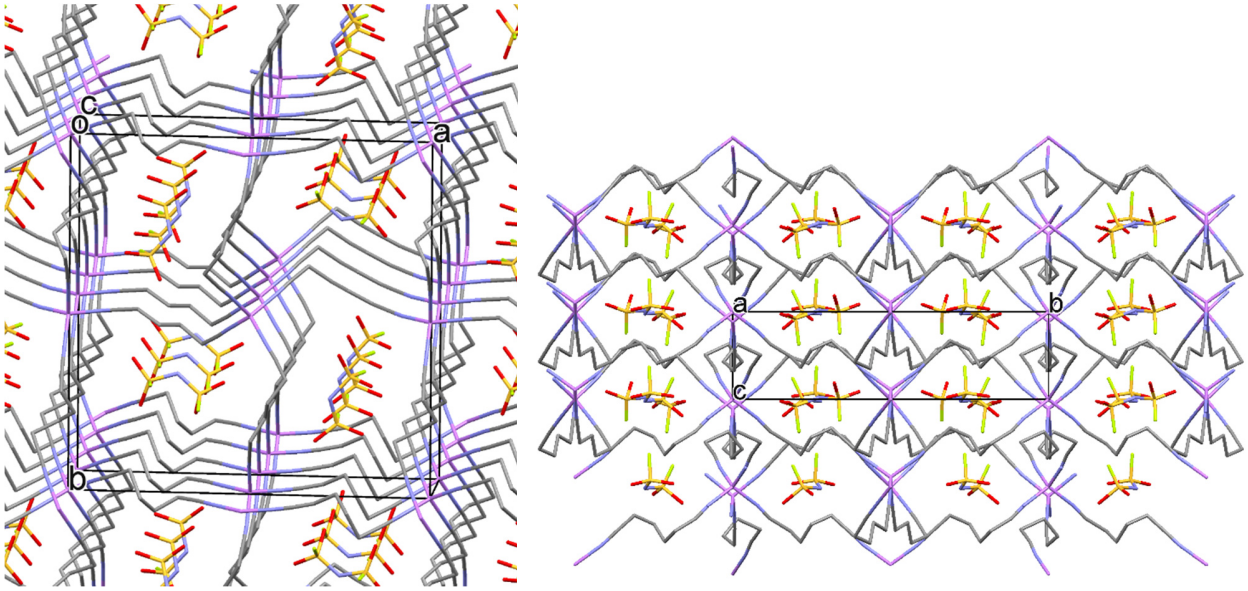

Figure S5. Packing diagram of LiFSA-$(ADN)_2$ crystals (two views). Hydrogen atoms are not shown. Purple, Li; red, O; gray, C; yellow, S; light green, F; lite blue, N. Single crystal of LiFSA-$(ADN)_2$ was successfully grown in the liquid of [LiFSA]/[ADN] = 1/10 at room temperature.

Table S3. Crystallographic data of LiFSA-$(ADN)_2$ crystal

	[LiFSA]/[ADN] = 1/2
Chemical formula	$C_{12}H_{16}F_2LiN_5O_4S_2$
Formula weight	403.36
Crystal system	tetragonal
Space group	$P\bar{4}$ (No81)
a / Å	18.955(2)
b / Å	18.955(2)
c / Å	5.2356(7)
α / °	90
β / °	90
γ / °	90
V / Å^3	1881.2(5)
Z	4
D_{calc} / g cm^{-3}	1.424
μ / mm^{-1}	0.329
Temp. / K	223
Reflections collected	3823
Independent reflection, R_{int}	2728
R_1 [I > 2σ(I)]	0.0530
wR_2 (all data)	0.1393
Goodness of fit	1.063

*The precision of the analysis is not sufficient for registration with Cambridge Structural Database (CSD), thus, the LiFSA-$(ADN)_2$ crystal have no CCDC number.

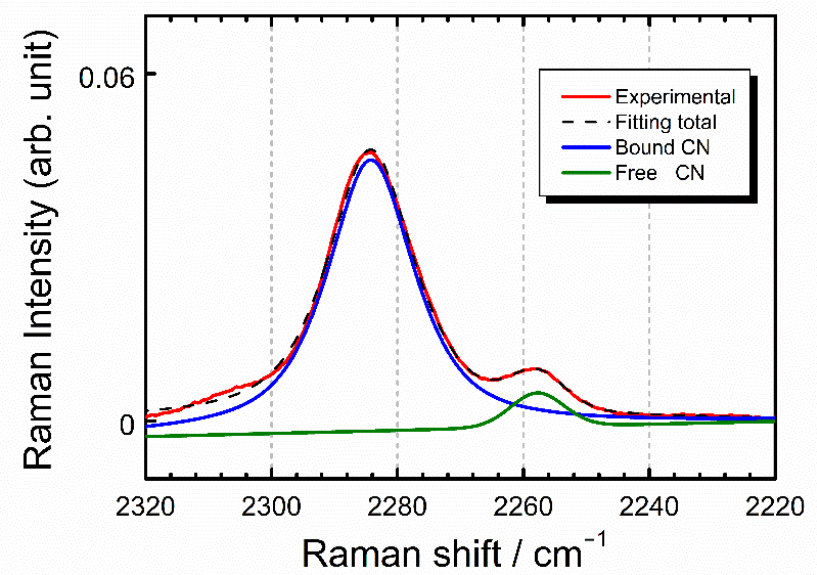

Figure S6. Raman spectrum of C≡N group of SN in [LiFSA]/[SN] = 1/0.8 in the range of 2220−2320 cm^{-1} measured at 60 °C. The spectrum was deconvoluted into the 2 peaks using the Gaussian−Lorentzian (pseudo-Voigt) function.

Table S4. The relative areas of Raman peaks of bound and free cyano groups in [LiFSA]/[SN] = 1/0.8.

	Bound CN / %	Free CN / %
[LiFSA]/[SN] = 1/0.8 at 60 °C	94.5	5.5

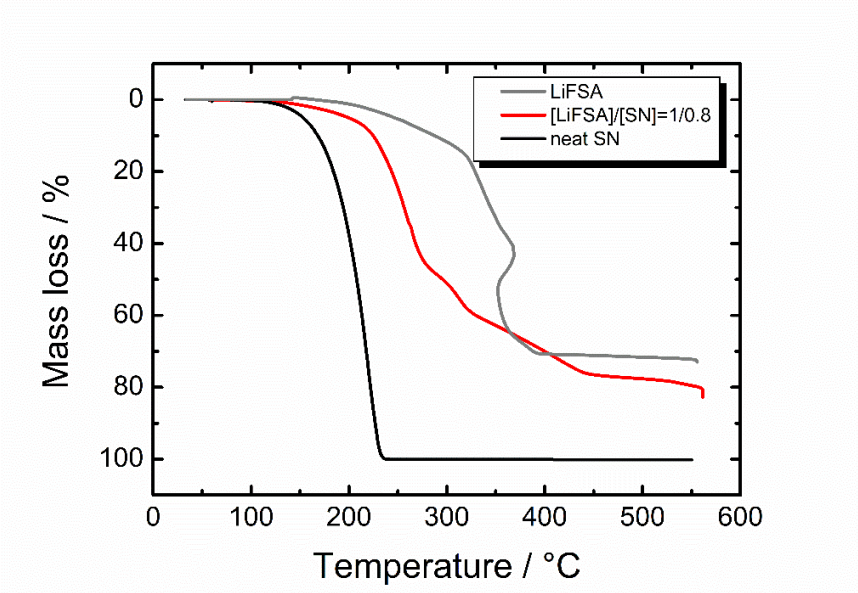

Figure S7. Thermogravimetric curves of [LiFSA]/[SN] = 1/0.8 and neat SN.

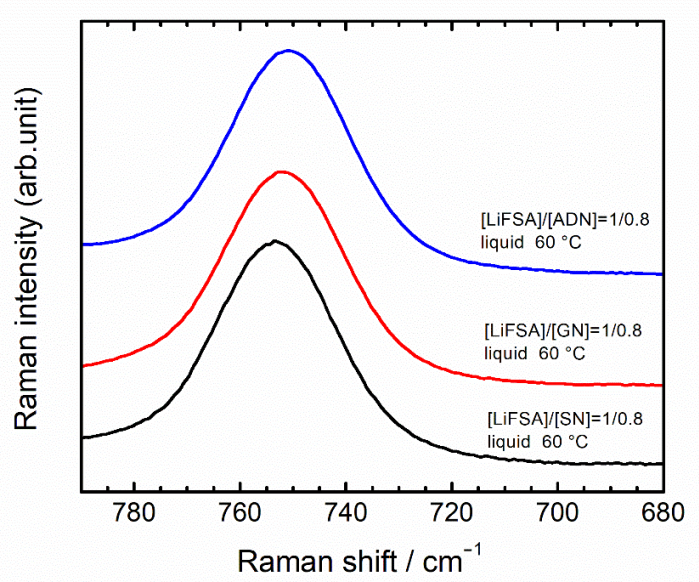

Figure S8. Raman spectra of FSA in [LiFSA]/[dinitrile] (SN, GN, ADN) = 1/0.8 measured at 60 °C.

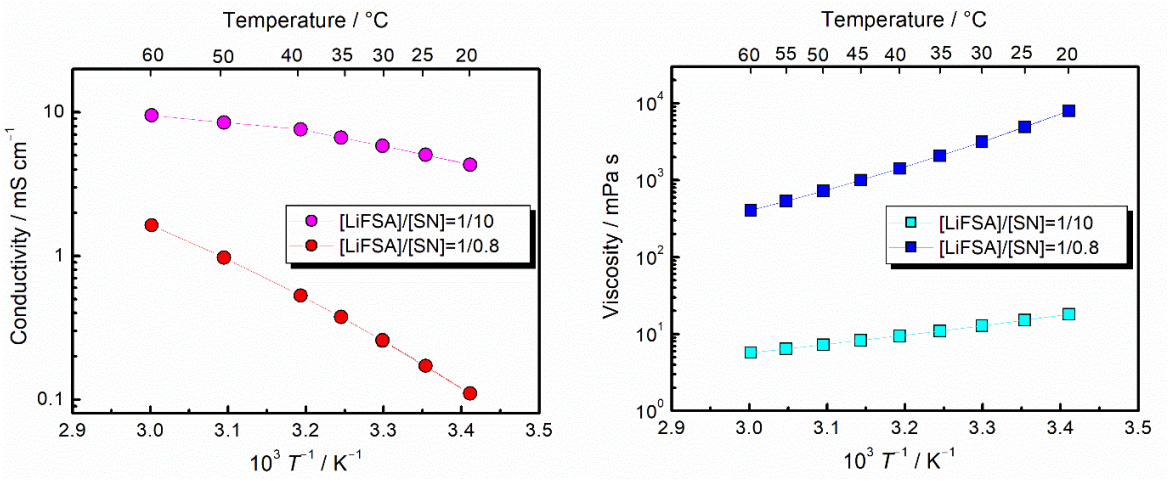

Figure S9. Temperature dependence of ionic conductivities and viscosities of [LiFSA]/[SN] = 1/0.8 and 1/10 electrolytes.

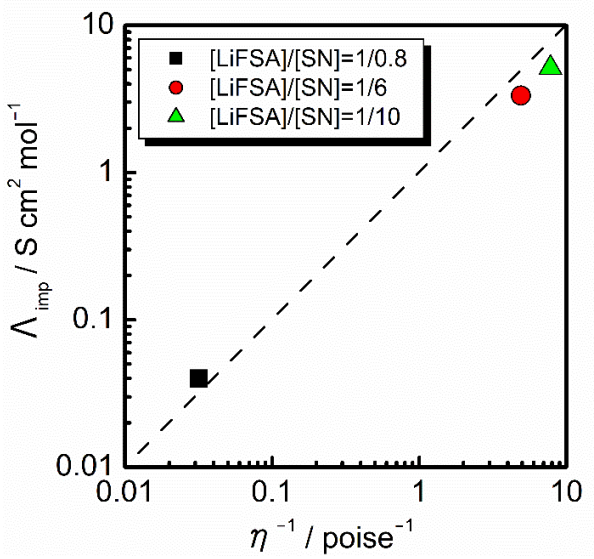

Figure S10. Walden plot for [LiFSA]/[SN] electrolytes at 30 °C.

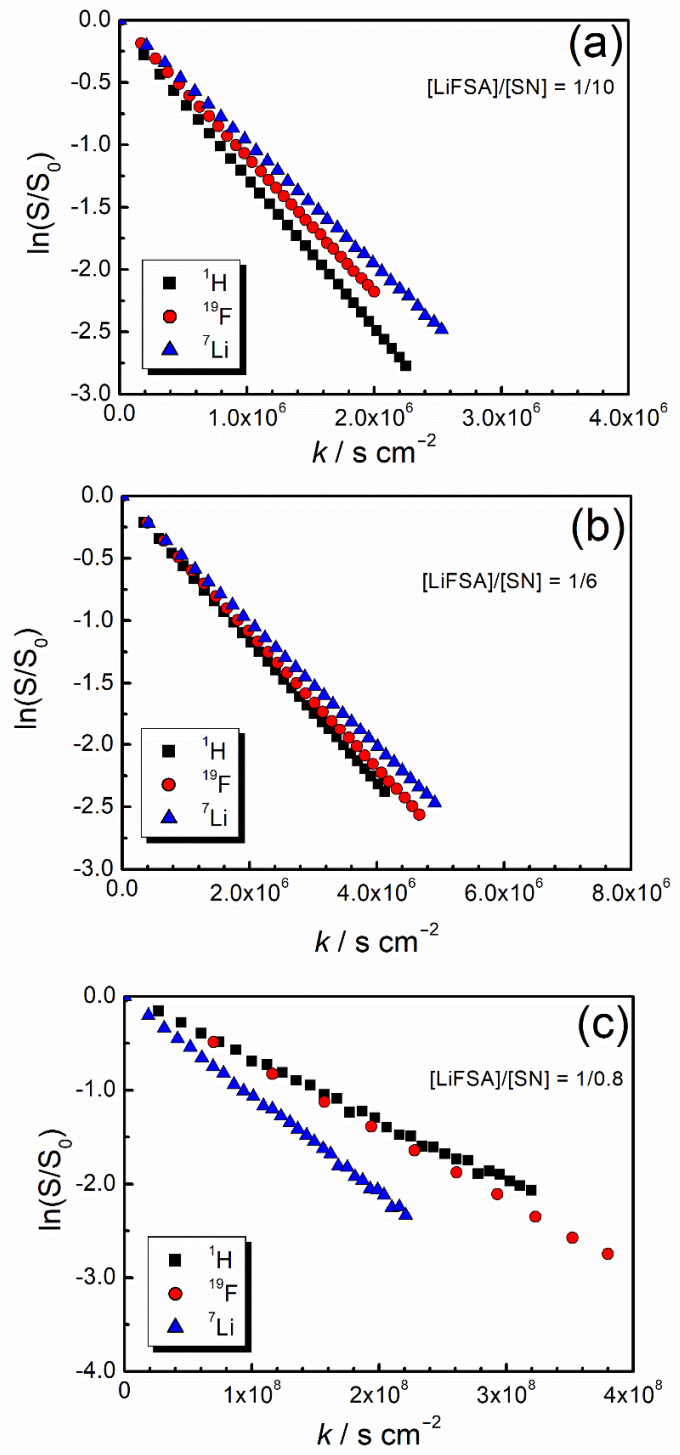

Figure S11. Plots of signal attenuation ln ($S/S_{\delta=0}$) versus $k = -4\gamma^2 g^2 \delta^2 (\Delta - 2\delta/3\pi - \tau_g/2)/\pi^2$ for ^{1}H, ^{19}F, and ^{7}Li PFG-NMR echo signals of LiFSA/SN mixtures measured at 30 °C.

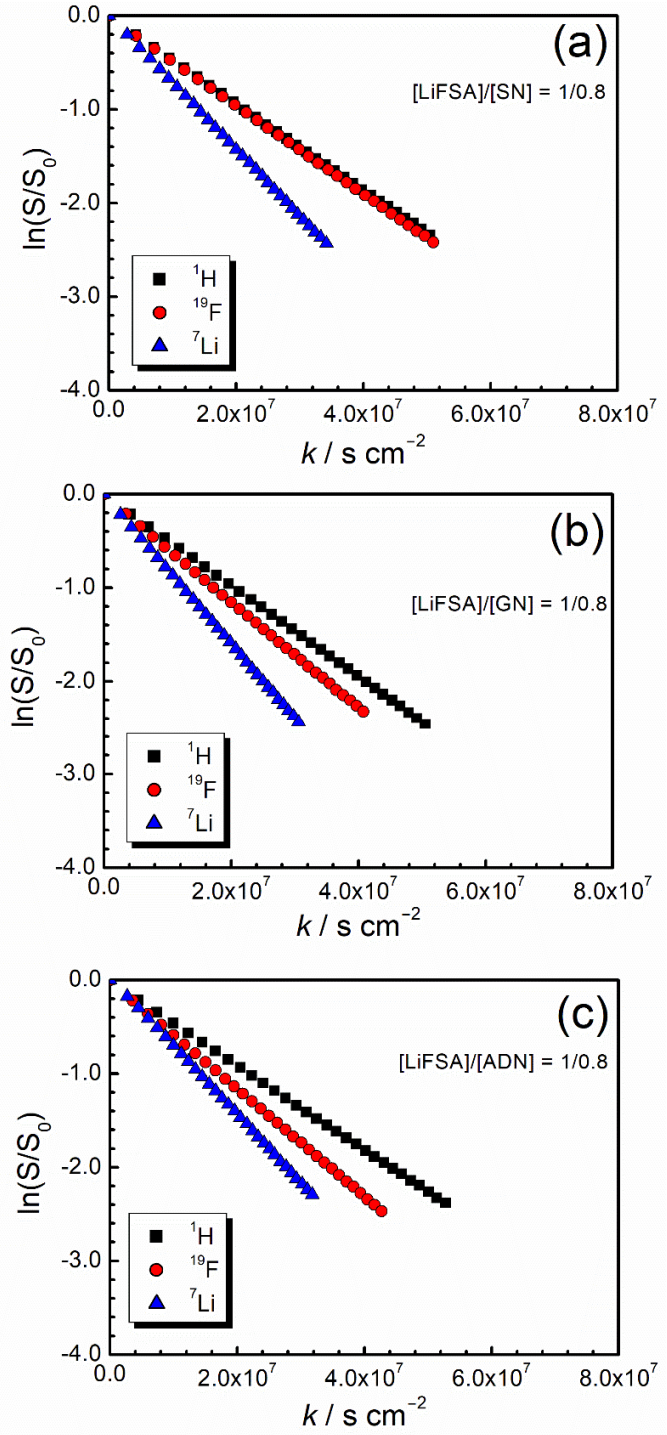

Figure S12. Plots of signal attenuation ln ($S/S_{\delta=0}$) versus $k = -4\gamma^2 g^2 \delta^2 (\Delta - 2\delta/3\pi - \tau_9/2)/\pi^2$ for ^{1}H, ^{19}F, and ^{7}Li PFG-NMR echo signals of [LiFSA]/[SN] = 1/0.8 (a), [LiFSA]/[GN] = 1/0.8 (b), and [LiFSA]/[ADN] = 1/0.8 (c) mixtures measured at 60 °C.

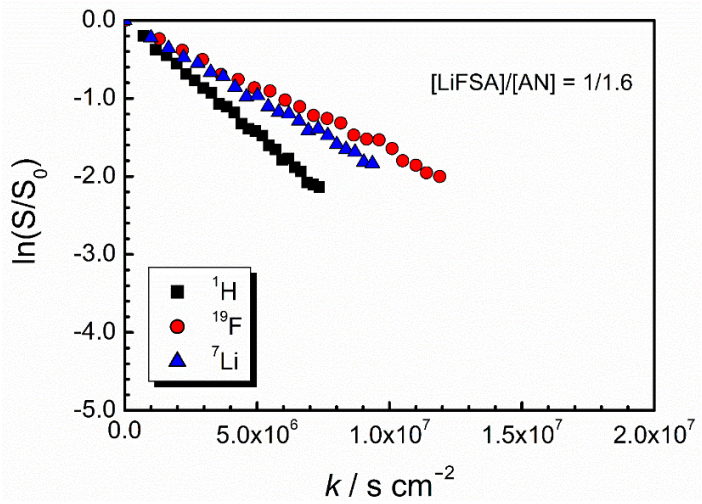

Figure S13. Plots of signal attenuation ln ($S/S_{\delta=0}$) versus $k = -4\gamma^2 g^2 \delta^2 (\Delta - 2\delta/3\pi - \tau_9/2)/\pi^2$ for ^{1}H, ^{19}F, and ^{7}Li PFG-NMR echo signals of [LiFSA]/[AN] = 1/1.6 mixture measured at 30 °C.

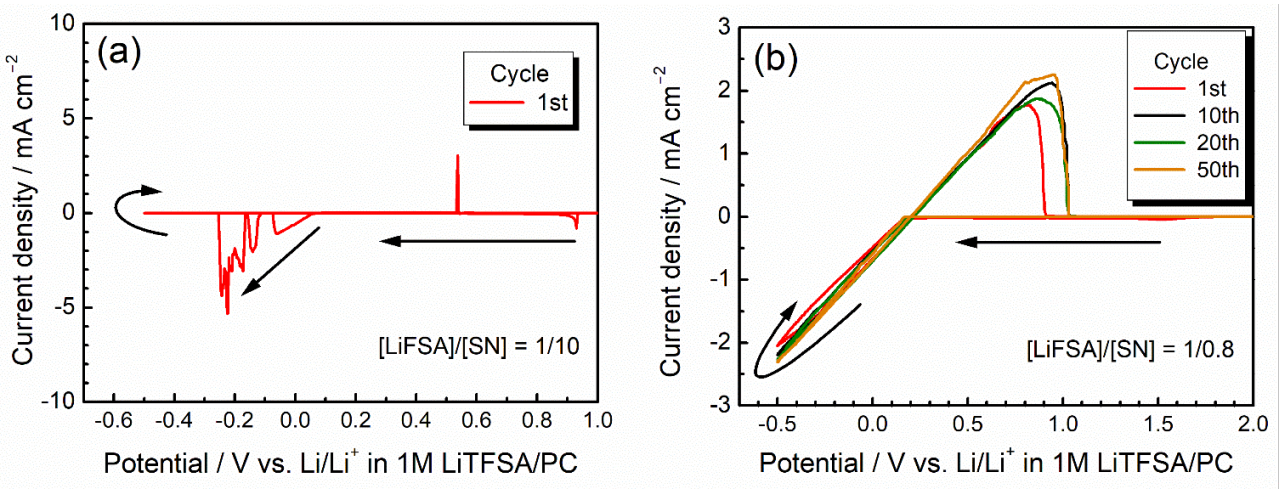

Figure S14. Cyclic voltammograms of [LiFSA]/[SN] = 1/10 (a) and 1/0.8 (b) electrolytes measured with a Cu electrode at a scan rate of 1 mV s^{-1} at 30 °C.

Transference Number of Li^+ Ion.

The transference number of Li^+ (t_{Li+}) can be estimated based on the electrochemical measurements for a symmetric [Li | electrolyte | Li] cell.[S1] The t_{Li+} is described as follows:

$$t_{Li^+} = \frac{I_{SS}(\Delta V - I_0 R_0)}{I_0(\Delta V - I_{SS} R_{SS})}$$

where I_{SS} is the steady-state current, I_0 is the initial current, and ΔV is the applied voltage to the cell. R_{SS} and R_0 are the electrode resistance after and before the polarization. In this study, the applied potential (ΔV) was 10 mV. Impedance spectra were collected before (0 s) and after (3600 s) the polarization, with sinusoidal alternating voltage amplitude of 10 mV (rms) and frequency ranging from 500 kHz to 1 Hz.

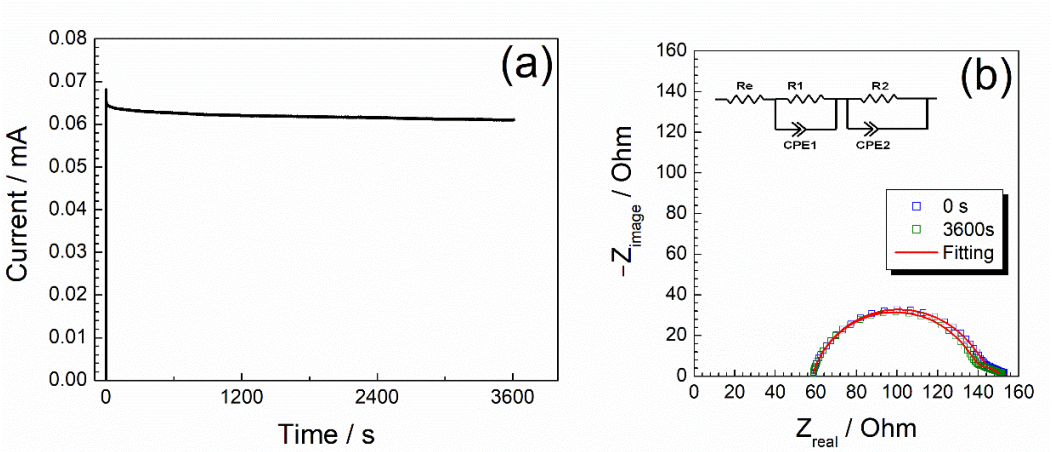

Figure S15. (a) Chronoamperogram and (b) Nyquist plots before and after the polarization for a symmetric [Li metal | [LiFSA]/[SN] = 1/0.8 with glass fiber filter separator (GA-55 (200 μm)) | Li metal] coin-type cell measured at 30 °C. The inset in (b) shows the equivalent circuit used in the fitting.

Table S5. Electrochemically estimated Li^+ transference numbers (t_{Li+}(EC)) from analysis of polarization experiments in the [Li | electrolyte with glass fiber filter separator (GA-55 (200 μm)) | Li] cell with [LiFSA]/[SN] = 1/0.8 electrolyte. For comparison, the transference number estimated from the self-diffusion coefficients, D_{Li} and D_{FSA}, (t_{Li+}(NMR)) is also shown.

molar ratio [LiFSA]/[SN]	I_0 mA	I_{SS} mA	R_0 Ω	R_{SS} Ω	t_{Li+}(EC) -	[a]t_{Li+}(NMR) -
1/0.8	0.068	0.061	94.3	92.9	0.74	0.62

[a] The t_{Li+}(NMR) was estimated from the self-diffusion coefficients of Li^+ (D_{Li}) and FSA^- (D_{FSA}):
$t_{Li+}(NMR) = D_{Li} / (D_{Li} + D_{FSA})$.

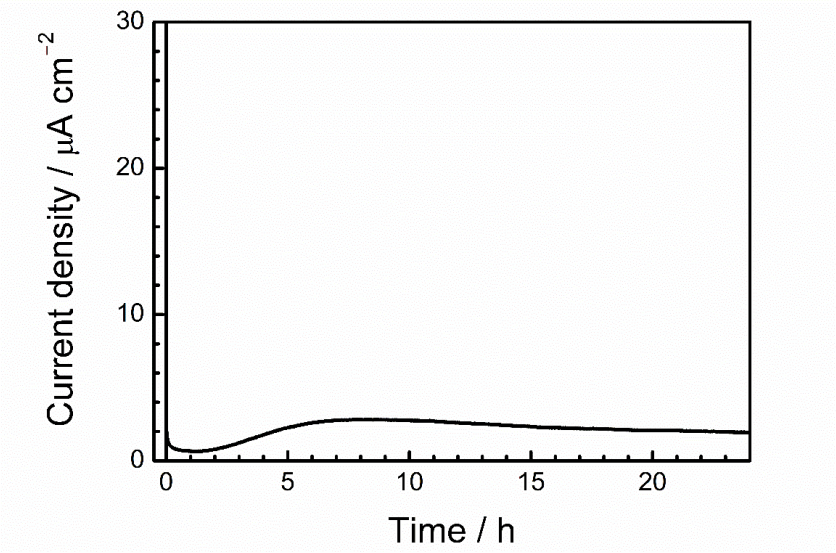

Figure S16. Chronoamperogram of an Al electrode recorded during prolonged polarization at 4.8 V vs Li/Li^+ in [LiFSA]/[SN] = 1/0.8 electrolyte at 30 °C. The measurement was carried out with a two-electrode cell (2032-type coin cell) using a Li metal foil as the counter electrode.

Reference for Supporting Information

(S1) J. Evans, C. A. Vincent, P. G. Bruce, *Polymer* **1987**, *28*, 2324–2328.